

Chapter 1

Characterizing Deep Gaussian Process Models

“On a given day, would I rather be wrestling with a sampler, or proving theorems?”

Peter Orbanz, personal communication

Choosing appropriate architectures and regularization strategies of deep networks is crucial to good predictive performance. To shed light on this problem, we analyze the analogous problem of constructing useful priors on compositions of functions. Specifically, we study the deep Gaussian process, a type of infinitely-wide, deep neural network. We show that in standard architectures, the representational capacity of the network tends to capture fewer degrees of freedom as the number of layers increases, retaining only a single degree of freedom in the limit. We propose an alternate network architecture which does not suffer from this pathology. We also examine deep covariance functions, obtained by composing infinitely many feature transforms. Lastly, we characterize the class of models obtained by performing dropout on Gaussian processes.

1.1 Introduction

Much recent work on deep networks has focused on weight initialization (Martens, 2010), regularization (Lee et al., 2007) and network architecture (Gens and Domingos, 2013). However, the interactions between these different design decisions can be complex and difficult to characterize. We propose to approach the design of deep architectures by examining the problem of assigning priors to nested compositions of functions. Well-

defined priors allow us to explicitly examine the assumptions being made about functions we may wish to learn. If we can identify classes of priors that give our models desirable properties, these in turn may suggest regularization, initialization, and architecture choices that also provide such properties.

Fundamentally, a multilayer neural network implements a composition of vector-valued functions, one per layer. Hence, understanding properties of such function compositions helps us gain insight into deep networks. In this paper, we examine a simple and flexible class of priors on compositions of functions, namely deep Gaussian processes (Damianou and Lawrence, 2013). Deep GPs are simply priors on compositions of vector-valued functions, where each output of each layer is drawn independently from a GP prior:

$$\mathbf{f}^{(1:L)}(\mathbf{x}) = \mathbf{f}^{(L)}(\mathbf{f}^{(L-1)}(\dots \mathbf{f}^{(2)}(\mathbf{f}^{(1)}(\mathbf{x}))\dots)) \quad (1.1)$$

$$\mathbf{f}_d^{(\ell)} \stackrel{\text{ind}}{\sim} \text{GP}\left(0, k_d^\ell(\mathbf{x}, \mathbf{x}')\right) \quad (1.2)$$

These models correspond to a certain type of infinitely-wide multi-layer perceptron (MLP), and as such make canonical candidates for generative models of functions that closely relate to neural networks.

By characterizing these models, this paper shows that representations based on repeated composition of independently-initialized functions exhibit a pathology where the representation becomes invariant to all but one direction of variation. This corresponds to an eventual debilitating decrease in the information capacity of networks as a function of their number of layers. However, we will demonstrate that a simple change in architecture — namely, connecting the input to each layer — fixes this problem.

We also present two related analyses: first, we examine the properties of a arbitrarily deep fixed feature transforms (“deep kernels”). Second, we characterise the prior obtained by performing dropout on GPs, showing equivalences to existing models.

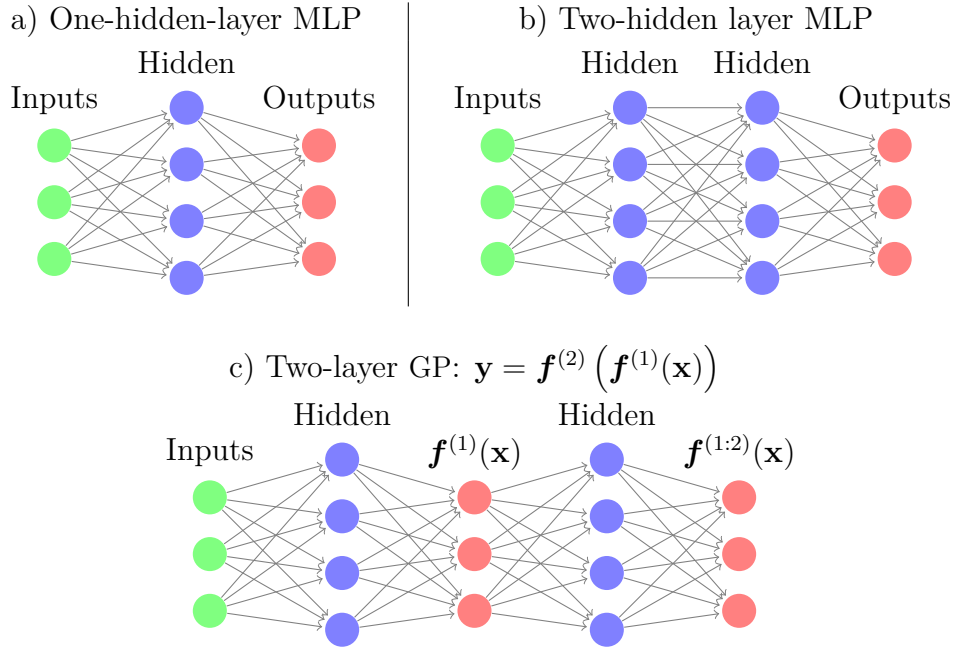


Fig. 1.1 a): GPs can be understood as a one-hidden-layer MLP with infinitely many hidden units. There are two interpretations of deep GPs as neural networks: b): As a neural network with a finite number of hidden units, each with a different non-parametric activation function. c) Alternatively, we can consider every second layer to be a random linear combination of an infinite number of fixed, parametric hidden units.

1.2 Relating Deep Neural Nets and Deep Gaussian Processes

1.2.1 Single-layer Models

In the typical definition of an MLP, the hidden units of the first layer are defined as:

$$\mathbf{h}^{(1)}(\mathbf{x}) = \sigma(\mathbf{b}^{(1)} + \mathbf{W}^{(1)}\mathbf{x}) \quad (1.3)$$

where \mathbf{h} are the hidden unit activations, \mathbf{b} is a bias vector, \mathbf{W} is a weight matrix and σ is a one-dimensional nonlinear function applied element-wise. The output vector $f(\mathbf{x})$ is simply a weighted sum of these hidden unit activations:

$$f(\mathbf{x}) = \mathbf{V}^{(1)}\sigma(\mathbf{b}^{(1)} + \mathbf{W}^{(1)}\mathbf{x}) = \mathbf{V}^{(1)}\mathbf{h}^{(1)}(\mathbf{x}) \quad (1.4)$$

where $\mathbf{V}^{(1)}$ is another weight matrix.

There exists a correspondence between one-layer MLPs and GPs (Neal, 1995). GPs can be viewed as a prior on neural networks with infinitely many hidden units, and unknown weights. More precisely, for any model of the form

$$f(\mathbf{x}) = \frac{1}{K} \boldsymbol{\alpha}^\top \mathbf{h}(\mathbf{x}) = \frac{1}{K} \sum_{i=1}^K \alpha_i h_i(\mathbf{x}), \quad (1.5)$$

with fixed features $[h_1(\mathbf{x}), \dots, h_K(\mathbf{x})]^\top = \mathbf{h}(\mathbf{x})$ and i.i.d. α 's with zero mean and finite variance σ^2 , the central limit theorem implies that as the number of features K grows, any two function values $f(\mathbf{x}), f(\mathbf{x}')$ have a joint distribution approaching $\mathcal{N}\left(0, \frac{\sigma^2}{K} \sum_{i=1}^K h_i(\mathbf{x})h_i(\mathbf{x}')\right)$. A joint Gaussian distribution between any set of function values is the definition of a Gaussian process.

The result is surprisingly general: it puts no constraints on the features (other than having uniformly bounded activation), nor does it require that the feature weights α be Gaussian distributed.

We can also work backwards to derive a one-layer MLP from any GP. Mercer's theorem implies that any positive-definite kernel function corresponds to an inner product of features: $k(\mathbf{x}, \mathbf{x}') = \mathbf{h}(\mathbf{x})^\top \mathbf{h}(\mathbf{x}')$. Thus in the one-hidden-layer case, the correspondence between MLPs and GPs is simple: the features $\mathbf{h}(\mathbf{x})$ of the kernel correspond to the hidden units of the MLP.

1.2.2 Multiple Hidden Layers

In an MLP, the ℓ th layer units are given by the recurrence

$$\mathbf{h}^{(\ell)}(\mathbf{x}) = \sigma \left(\mathbf{b}^{(\ell)} + \mathbf{W}^{(\ell)} \mathbf{h}^{(\ell-1)}(\mathbf{x}) \right) . \quad (1.6)$$

This architecture is shown in figure 1.1b. For example, if we extend the model given by (1.4) to have two layers of feature mappings, the resulting model is

$$f(\mathbf{x}) = \frac{1}{K} \boldsymbol{\alpha}^\top \mathbf{h}^{(2)} \left(\mathbf{h}^{(1)}(\mathbf{x}) \right) . \quad (1.7)$$

If the features $\mathbf{h}(\mathbf{x})$ are considered fixed with only the last layer weights $\boldsymbol{\alpha}$ unknown, this model corresponds to a GP with a “deep kernel”:

$$k(\mathbf{x}, \mathbf{x}') = \left(\mathbf{h}^{(2)}(\mathbf{h}^{(1)}(\mathbf{x})) \right)^\top \mathbf{h}^{(2)}(\mathbf{h}^{(1)}(\mathbf{x}')) \quad (1.8)$$

These models, examined in section 1.6, imply a fixed representation as opposed to a prior over representations, which is what we wish to analyze in this paper.

To construct a neural network with fixed nonlinearities corresponding to a deep GP, one must introduce a second layer in between each infinitely-wide set of fixed basis functions, as in figure 1.1c. The D_ℓ outputs $\mathbf{f}^{(\ell)}(\mathbf{x})$ in between each layer are weighted sums (with unknown weights) of the fixed hidden units of the layer below, and the next layer’s hidden units depend only on these D_ℓ outputs.

This alternating-layer architecture has an interpretation as a series of linear information bottlenecks. We can simply substitute (1.4) into (1.6) to get

$$\mathbf{h}^{(\ell)}(\mathbf{x}) = \sigma \left(\mathbf{b}^{(\ell)} + \mathbf{W}^{(\ell)} \mathbf{V}^{(\ell-1)} \mathbf{h}^{(\ell-1)}(\mathbf{x}) \right). \quad (1.9)$$

Thus, ignoring the intermediate outputs $\mathbf{f}^{(\ell)}(\mathbf{x})$, a deep GP is an infinitely-wide, deep MLP with each pair of layers connected by random, rank- D_ℓ matrices $\mathbf{W}^{(\ell)} \mathbf{V}^{(\ell-1)}$.

A more direct way to construct a network architecture corresponding to a deep GP is to integrate out all $\mathbf{V}^{(\ell)}$, and view deep GPs as a neural network with a finite number of nonparametric, GP-distributed basis functions at each layer, in which $\mathbf{f}^{(1:\ell)}(\mathbf{x})$ represent the output of the hidden nodes at the ℓ^{th} layer. This second view lets us compare deep GP models to standard neural net architectures more directly.

1.3 Characterizing Deep Gaussian Processes

In this section, we develop several theoretical results that explore the behavior of deep GPs as a function of their depth. This will allow us in section 1.4 to formally identify a pathology that emerges in very deep networks.

Specifically, we will show that the size of the derivative of a one-dimensional deep GP becomes log-normal distributed as the network becomes deeper. We’ll also show that the Jacobian of a multivariate deep GP is a product of independent Gaussian matrices with independent entries.

1.3.1 One-dimensional Asymptotics

In this section, we derive the limiting distribution of the derivative of an arbitrarily deep, one-dimensional GP with a squared-exp kernel:

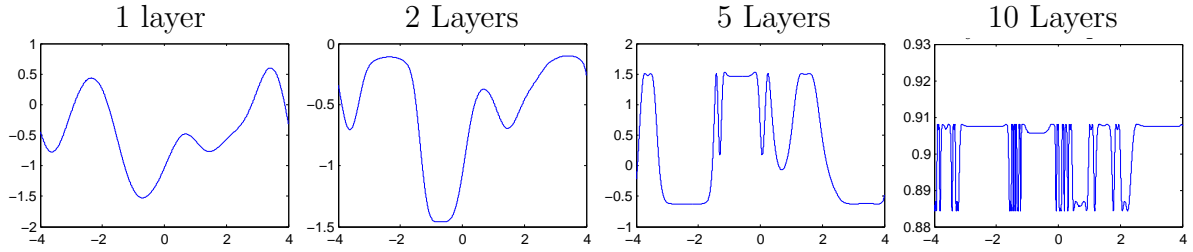


Fig. 1.2 One-dimensional draws from a deep gp prior. After a few layers, the functions begin to be either nearly flat, or highly varying, everywhere. This is a consequence of the distribution on derivatives becoming heavy-tailed.

$$k_{\text{SE}}(x, x') = \sigma^2 \exp\left(\frac{-(x - x')^2}{2w^2}\right). \quad (1.10)$$

The hyperparameter σ^2 controls the variance of functions drawn from the prior, and the hyperparameter w controls the smoothness. The derivative of a GP with a squared-exp kernel is pointwise distributed as $\mathcal{N}(0, \sigma^2/w^2)$. Intuitively, a GP is likely to have large derivatives if it has high variance and small lengthscales.

By the chain rule, the derivative of a one-dimensional deep GP is simply a product of its (independent) derivatives. The distribution of the absolute value of this derivative is a product of half-normals, each with mean $\sqrt{2\sigma^2/\pi w^2}$.

If we choose kernel parameters so that $\sigma^2/w^2 = \pi/2$, then the expected magnitude of the derivative remains constant regardless of the depth.

The log of the magnitude of the derivatives has moments

$$\begin{aligned} m_{\log} &= \mathbb{E} \left[\log \left| \frac{\partial f(x)}{\partial x} \right| \right] = 2 \log \left(\frac{\sigma}{w} \right) - \log 2 - \gamma \\ v_{\log} &= \mathbb{V} \left[\log \left| \frac{\partial f(x)}{\partial x} \right| \right] = \frac{\pi^2}{4} + \frac{\log^2 2}{2} - \gamma^2 - \gamma \log 4 + 2 \log \left(\frac{\sigma}{w} \right) \left[\gamma + \log 2 - \log \left(\frac{\sigma}{w} \right) \right] \end{aligned} \quad (1.11)$$

where $\gamma \approx 0.5772$ is Euler's constant. Since the second moment is finite, by the central limit theorem, the limiting distribution of the size of the gradient approaches log-normal

as L grows:

$$\begin{aligned} \log \left| \frac{\partial f^{(1:L)}(x)}{\partial x} \right| &= \sum_{\ell=1}^L \log \left| \frac{\partial f^{(\ell)}(x)}{\partial x} \right| \\ \implies \log \left| \frac{\partial f^{(1:L)}(x)}{\partial x} \right| &\stackrel{L \rightarrow \infty}{\sim} \mathcal{N}(Lm_{\log}, L^2 v_{\log}) \end{aligned} \quad (1.12)$$

Even if the expected magnitude of the derivative remains constant, the variance of the log-normal distribution grows without bound as the depth increases. Because the log-normal distribution is heavy-tailed and its domain is bounded below by zero, the derivative will become very small almost everywhere, with rare but very large jumps.

Figure 1.2 shows this behavior in a draw from a 1D deep GP prior, at varying depths. This figure also shows that once the derivative in one region of the input space becomes very large or very small, it is likely to remain that way in subsequent layers.

1.3.2 Distribution of the Jacobian

We now derive the distribution on Jacobians of multivariate functions drawn from a deep GP prior.

Lemma 1.3.1. *The partial derivatives of a function mapping $\mathbb{R}^D \rightarrow \mathbb{R}$ drawn from a GP prior with a product kernel are independently Gaussian distributed.*

Proof. Because differentiation is a linear operator, the derivatives of a function drawn from a GP prior are also jointly Gaussian distributed. The covariance between partial derivatives w.r.t. input dimensions d_1 and d_2 of vector \mathbf{x} are given by Solak et al. (2003):

$$\text{cov} \left(\frac{\partial f(\mathbf{x})}{\partial x_{d_1}}, \frac{\partial f(\mathbf{x})}{\partial x_{d_2}} \right) = \frac{\partial^2 k(\mathbf{x}, \mathbf{x}')}{\partial x_{d_1} \partial x'_{d_2}} \Big|_{\mathbf{x}=\mathbf{x}'} \quad (1.13)$$

If our kernel is a product over individual dimensions $k(\mathbf{x}, \mathbf{x}') = \prod_d^D k_d(x_d, x'_d)$, as in the case of the squared-exp kernel, then the off-diagonal entries are zero, implying that all elements are independent. \square

In the case of the multivariate squared-exp kernel, the covariance between derivatives

has the form:

$$\begin{aligned} f(\mathbf{x}) &\sim \text{GP} \left(0, \sigma^2 \prod_{d=1}^D \exp \left(-\frac{1}{2} \frac{(x_d - x'_d)^2}{w_d^2} \right) \right) \\ \implies \text{cov} \left(\frac{\partial f(\mathbf{x})}{\partial x_{d_1}}, \frac{\partial f(\mathbf{x})}{\partial x_{d_2}} \right) &= \begin{cases} \frac{\sigma^2}{w_{d_1}^2} & \text{if } d_1 = d_2 \\ 0 & \text{if } d_1 \neq d_2 \end{cases} \end{aligned} \quad (1.14)$$

Lemma 1.3.2. *The Jacobian of a set of D functions $\mathbb{R}^D \rightarrow \mathbb{R}$ drawn independently from a GP prior with a product kernel is a $D \times D$ matrix of independent Gaussian R.V.'s*

Proof. The Jacobian of the vector-valued function $\mathbf{f}(\mathbf{x})$ is a matrix J with elements $J_{ij} = \frac{\partial f_i(\mathbf{x})}{\partial x_j}$. Because we've assumed that the GPs on each output dimension $f_d(\mathbf{x})$ are independent (1.2), it follows that each row of J is independent. Lemma 1.3.1 shows that the elements of each row are independent Gaussian. Thus all entries in the Jacobian of a GP-distributed transform are independent Gaussian R.V.'s. \square

Theorem 1.3.3. *The Jacobian of a deep GP with a product kernel is a product of independent Gaussian matrices, with each entry in each matrix being drawn independently.*

Proof. When composing L different functions, we'll denote the *immediate* Jacobian of the function mapping from layer $\ell - 1$ to layer ℓ as $J^\ell(\mathbf{x})$, and the Jacobian of the entire composition of L functions by $J^{1:L}(\mathbf{x})$. By the multivariate chain rule, the Jacobian of a composition of functions is simply the product of the immediate Jacobian matrices of each function. Thus the Jacobian of the composed (deep) function $\mathbf{f}^{(L)}(\mathbf{f}^{(L-1)}(\dots \mathbf{f}^{(3)}(\mathbf{f}^{(2)}(\mathbf{f}^{(1)}(\mathbf{x}))) \dots))$ is

$$J^{1:L}(\mathbf{x}) = J^L J^{(L-1)} \dots J^3 J^2 J^1. \quad (1.15)$$

By lemma 1.3.2, each $J_{i,j}^\ell \stackrel{\text{ind}}{\sim} \mathcal{N}$, so the complete Jacobian is a product of independent Gaussian matrices, with each entry of each matrix drawn independently. \square

Theorem 1.3.3 allows us to analyze the representational properties of a deep Gaussian process by simply examining the properties of products of independent Gaussian matrices, a well-studied object.

1.4 Formalizing a Pathology

Rifai et al. (2011a) argue that a good latent representation is invariant in directions orthogonal to the manifold on which the data lie. Conversely, a good latent representation

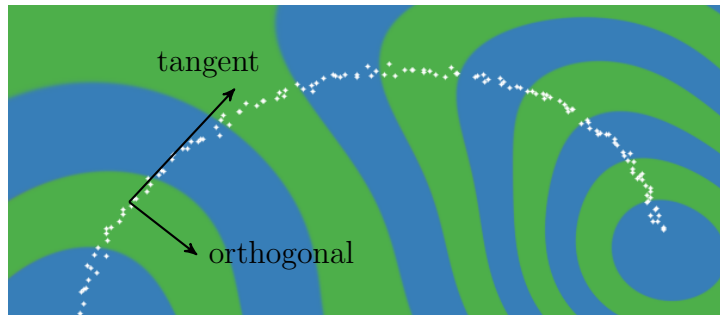


Fig. 1.3 Representing a 1-D data manifold. Colors correspond to the computed representation as a function of the input space. The representation (blue & green) varies in directions tangent to the data manifold (white), preserving information for later layers. The representation is also invariant to directions orthogonal to the manifold, making it robust to noise in those directions.

must also change in directions tangent to the data manifold, in order to preserve relevant information. Figure 1.3 visualizes this idea. As in Rifai et al. (2011b), we characterize the representational properties of a function by the singular value spectrum of the Jacobian. In their experiments, the Jacobian was computed at the training points. Because the priors we are examining are stationary, the distribution of the Jacobian is identical everywhere. Figure 1.4 shows the singular value spectrum for 5-dimensional deep GPs of different depths. As the net gets deeper, the largest singular value dominates, implying there is usually only one effective degree of freedom in representation being computed.

Figure 1.5 demonstrates a related pathology that arises when composing functions to produce a deep density model. The density in the observed space eventually becomes locally concentrated onto one-dimensional manifolds, or *filaments*, implying that such models are unsuitable to model manifolds whose underlying dimensionality is greater than one.

To visualize this pathology in another way, figure 1.6 illustrates a colour-coding of the representation computed by a deep GP, evaluated at each point in the input space. After 10 layers, we can see that locally, there is usually only one direction that one can move in \mathbf{x} -space in order to change the value of the computed representation. This means that such representations are likely to be unsuitable for decision tasks that depend on more than one property of the input.

To what extent are these pathologies present in nets being used today? In simulations, we found that for deep functions with a fixed latent dimension D , the singular value spectrum remained relatively flat for hundreds of layers as long as $D > 100$. Thus,

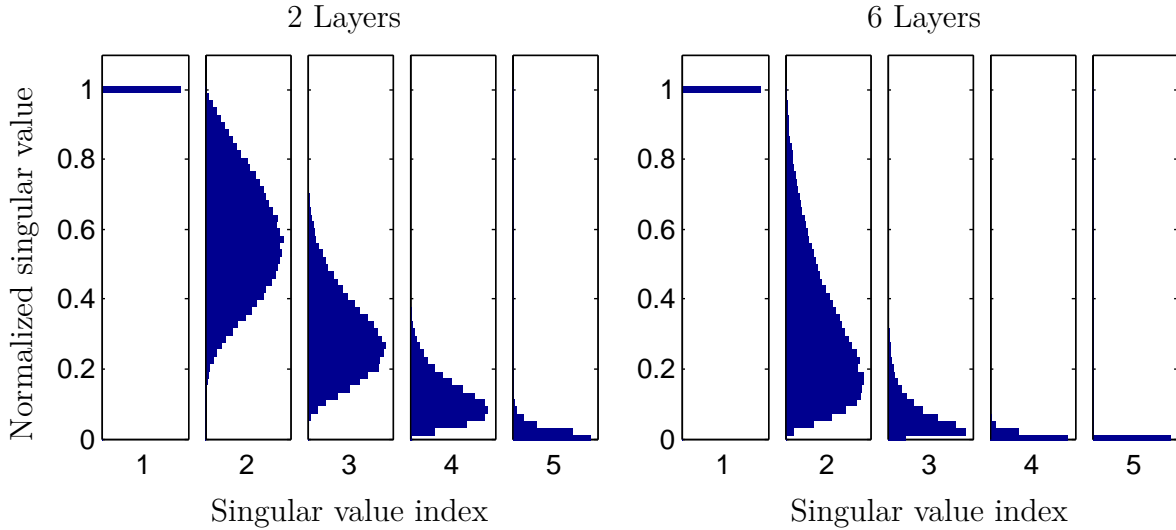


Fig. 1.4 The distribution of singular values relative to the largest, of the Jacobian of a function drawn from 5-dimensional deep GP prior, at 25 and 50 layers deep. As the net gets deeper, the largest singular value becomes much larger than the others. This implies that with high probability, there is only one effective degree of freedom in the representation being computed.

these pathologies are unlikely to severely affect relatively shallow, wide networks.

1.5 Fixing the Pathology

Following a suggestion from [Neal \(1995\)](#), we can fix the pathologies exhibited in figures 1.5 and 1.6 by simply making each layer depend not only on the output of the previous layer, but also on the original input \mathbf{x} . We refer to these models as *input-connected* networks. Figure 1.7 shows a graphical representation of the two connectivity architectures. Similar connections between non-adjacent layers can also be found in the primate visual cortex ([Maunsell and van Essen, 1983](#)). Formally, this functional dependence can be written as

$$\mathbf{f}^{(1:L)}(\mathbf{x}) = \mathbf{f}^{(L)} \left(\mathbf{f}^{(1:L-1)}(\mathbf{x}), \mathbf{x} \right), \quad \forall L \quad (1.16)$$

Draws from the resulting prior are shown in figures 1.8, 1.9 and 1.11. The Jacobian

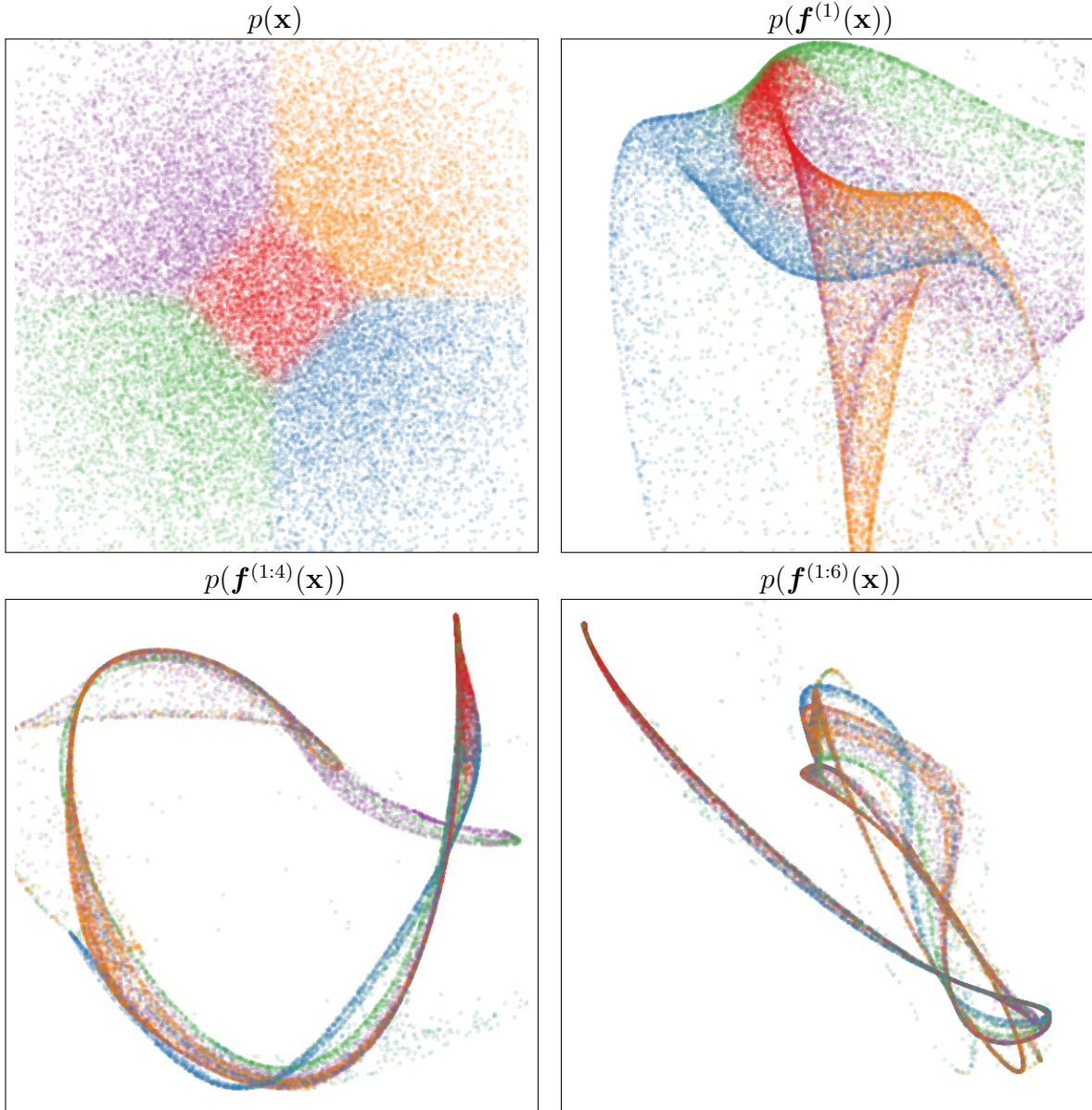


Fig. 1.5 Visualization of draws from a deep GP. A 2-dimensional Gaussian distribution (top left) is warped by successive functions drawn from a GP prior. As the number of layers increases, the density concentrates along one-dimensional filaments.

of the composed, input-connected deep function is defined by the recurrence

$$J^{1:L}(\mathbf{x}) = J^L \begin{bmatrix} J^{1:L-1} \\ I_D \end{bmatrix}. \quad (1.17)$$

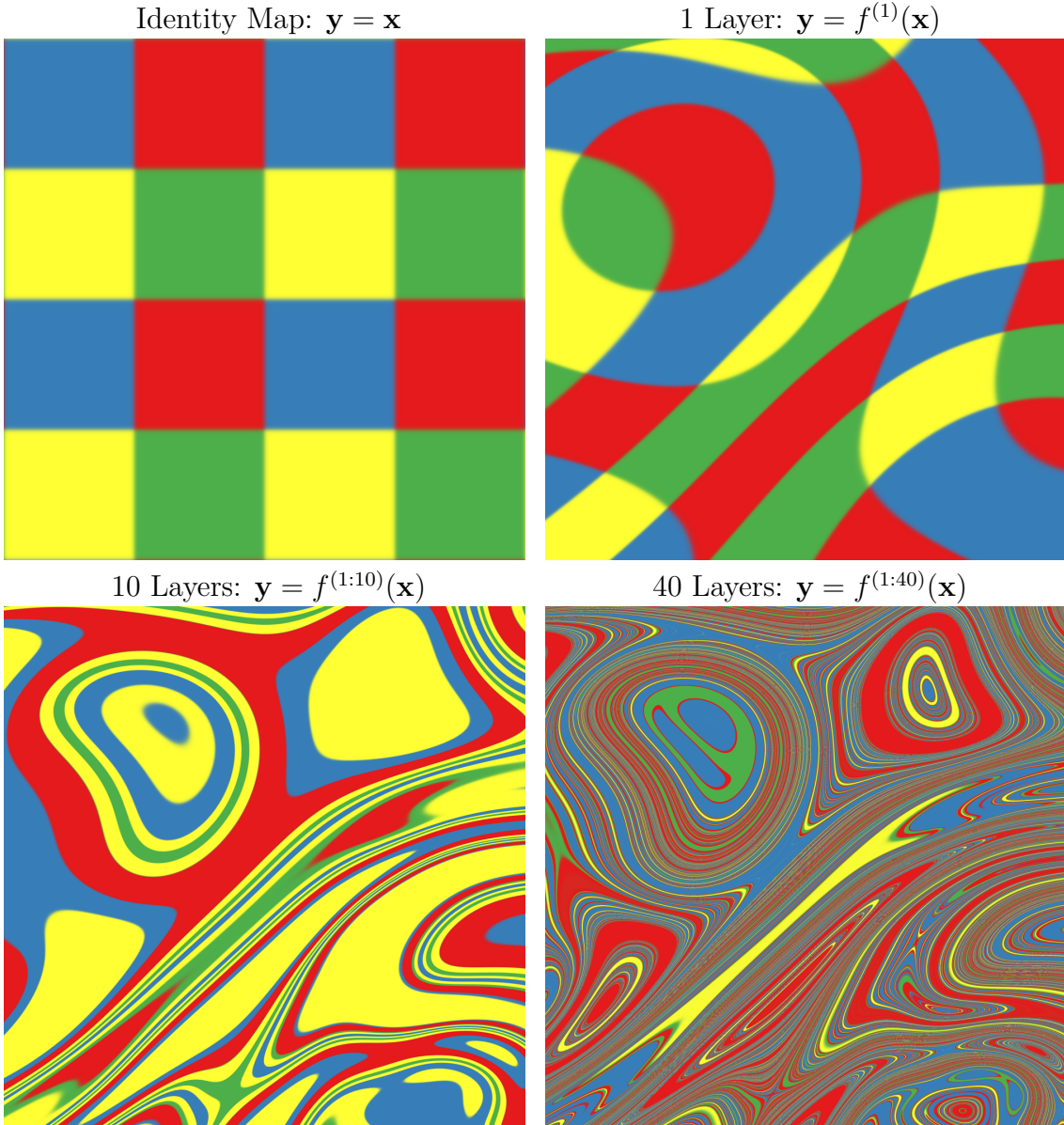


Fig. 1.6 Feature mapping of a deep GP. Colors correspond to the location $\mathbf{y} = \mathbf{f}(\mathbf{x})$ that each point is mapped to after being warped by a deep GP. The number of directions in which the color changes rapidly corresponds to the number of large singular values in the Jacobian. Just as the densities in figure 1.5 became locally one-dimensional, there is usually only one direction that one can move \mathbf{x} in locally to change \mathbf{y} . This means that \mathbf{f} is unlikely to be a suitable representation for decision tasks that depend on more than one aspect of \mathbf{x} .

Figure 1.10 shows that with this architecture, even 50-layer deep GPs have well-behaved singular value spectra.

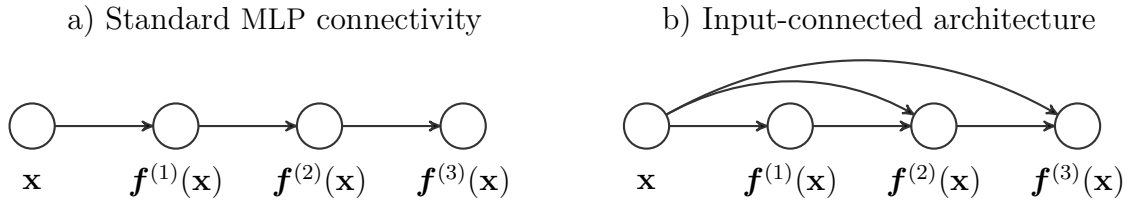


Fig. 1.7 Two different architectures for deep neural networks. The standard architecture connects each layer's outputs to the next layer's inputs. The input-connected architecture also connects the original input \mathbf{x} to each layer.

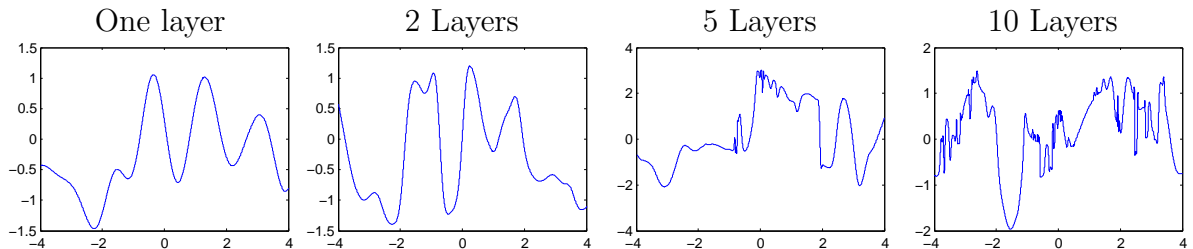


Fig. 1.8 Draws from a 1D deep GP prior with each layer connected to the input. Even after many layers, the functions remain smooth in some regions, while varying rapidly in other regions. Compare to standard-connectivity deep GP draws shown in figure 1.2.

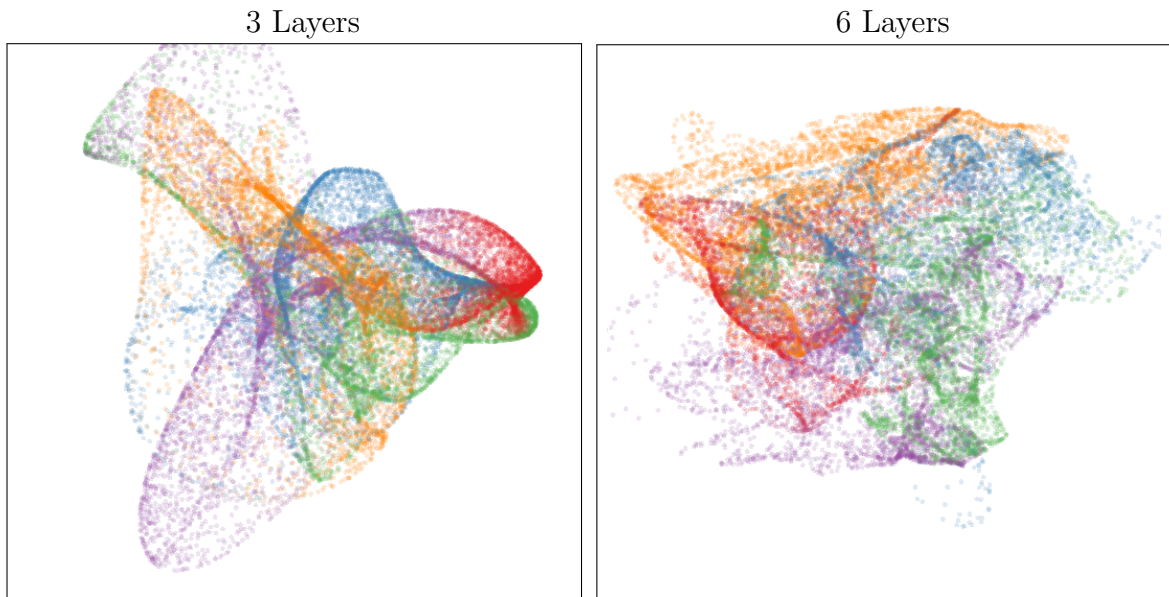


Fig. 1.9 Left: Densities defined by a draw from a deep GP, with each layer connected to the input \mathbf{x} . As depth increases, the density becomes more complex without concentrating along filaments.

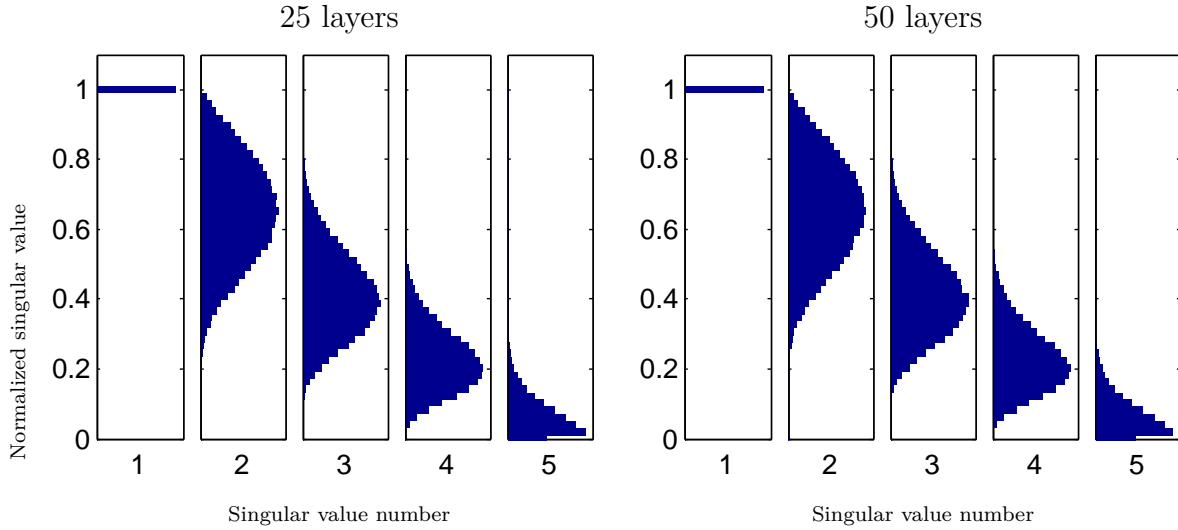


Fig. 1.10 The distribution of singular values drawn from 5-dimensional input-connected deep GP priors, 25 and 50 layers deep. The singular values remain roughly the same scale as one another.

1.6 Deep Kernels

Bengio et al. (2006) showed that kernel machines have limited generalization ability when they use a local kernel such as the squared-exp. However, many interesting non-local kernels can be constructed which allow non-trivial extrapolation. For example, periodic kernels can be viewed as a 2-layer-deep kernel, in which the first layer maps $x \rightarrow [\sin(x), \cos(x)]$, and the second layer maps through basis functions corresponding to the SE kernel.

Can we construct other useful kernels by composing fixed feature maps several times, creating deep kernels? Cho (2012) constructed kernels of this form, repeatedly applying multiple layers of feature mappings. We can compose the feature mapping of two kernels:

$$k_1(\mathbf{x}, \mathbf{x}') = \mathbf{h}_1(\mathbf{x})^\top \mathbf{h}_1(\mathbf{x}') \quad (1.18)$$

$$k_2(\mathbf{x}, \mathbf{x}') = \mathbf{h}_2(\mathbf{x})^\top \mathbf{h}_2(\mathbf{x}') \quad (1.19)$$

$$(k_1 \circ k_2)(\mathbf{x}, \mathbf{x}') = k_2(\mathbf{h}_1(\mathbf{x}), \mathbf{h}_1(\mathbf{x}')) \quad (1.20)$$

$$= [\mathbf{h}_2(\mathbf{h}_1(\mathbf{x}))]^\top \mathbf{h}_2(\mathbf{h}_1(\mathbf{x}')) \quad (1.21)$$

Composing the squared-exp kernel with any implicit mapping $\mathbf{h}(\mathbf{x})$ has a simple

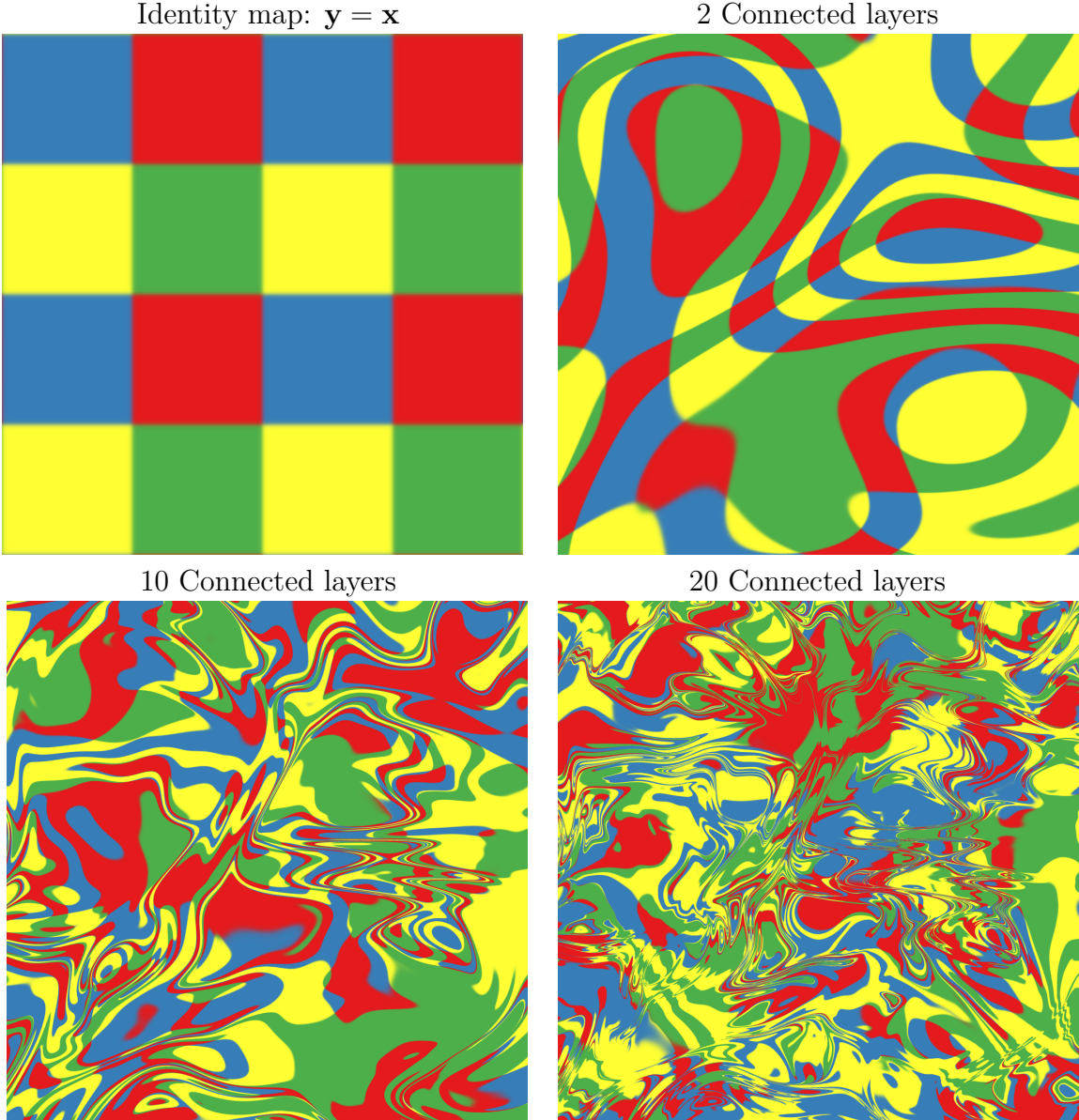


Fig. 1.11 Feature mapping of a deep GP with each layer connected to the input \mathbf{x} . Just as the densities in figure 1.9 remained locally two-dimensional even after many transformations, in this mapping there are often two directions that one can move locally in \mathbf{x} to in order to change the values of $f(\mathbf{x})$. This means that the prior puts mass on representations which sometimes depend on all aspects of the input. Compare to figure 1.6.

closed form:

$$\begin{aligned}
 k_{L+1}(\mathbf{x}, \mathbf{x}') &= k_{SE}(\mathbf{h}(\mathbf{x}), \mathbf{h}(\mathbf{x}')) = & (1.22) \\
 &= \exp\left(-\frac{1}{2}\|\mathbf{h}(\mathbf{x}) - \mathbf{h}(\mathbf{x}')\|_2^2\right) \\
 &= \exp\left(-\frac{1}{2}\left[\mathbf{h}(\mathbf{x})^\top \mathbf{h}(\mathbf{x}) - 2\mathbf{h}(\mathbf{x})^\top \mathbf{h}(\mathbf{x}') + \mathbf{h}(\mathbf{x}')^\top \mathbf{h}(\mathbf{x}')\right]\right) \\
 &= \exp\left(-\frac{1}{2}[k_L(\mathbf{x}, \mathbf{x}) - 2k_L(\mathbf{x}, \mathbf{x}') + k_L(\mathbf{x}', \mathbf{x}')]\right)
 \end{aligned}$$

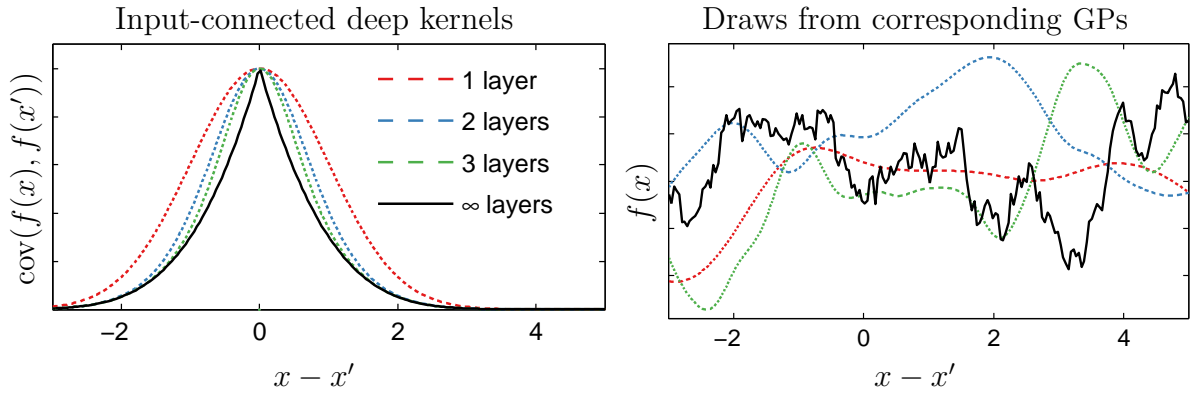


Fig. 1.12 Left: Input-connected deep kernels. By connecting the inputs \mathbf{x} to each layer, the kernel can still depend on its input even after arbitrarily many layers of computation. Right: GP draws using deep input-connected kernels.

Thus, we can express k_{L+1} exactly in terms of k_L .

1.6.1 Infinitely Deep Kernels

What happens when we repeat this composition of feature maps many times, starting with the squared-exp kernel? In the infinite limit, this recursion converges to $k(\mathbf{x}, \mathbf{x}') = 1$ for all pairs of inputs, which corresponds to a prior on constant functions $f(\mathbf{x}) = c$.

A non-degenerate construction As before, we can overcome this degeneracy by connecting the inputs \mathbf{x} to each layer. To do so, we simply augment the feature vector $\mathbf{h}_L(\mathbf{x})$ with \mathbf{x} at each layer:

$$\begin{aligned} k_{L+1}(\mathbf{x}, \mathbf{x}') &= \exp\left(-\frac{1}{2}\left\|\begin{bmatrix} \mathbf{h}_L(\mathbf{x}) \\ \mathbf{x} \end{bmatrix} - \begin{bmatrix} \mathbf{h}_L(\mathbf{x}') \\ \mathbf{x}' \end{bmatrix}\right\|_2^2\right) \\ &= \exp\left(-\frac{1}{2}[k_L(\mathbf{x}, \mathbf{x}) - 2k_L(\mathbf{x}, \mathbf{x}') + k_L(\mathbf{x}', \mathbf{x}') - \|\mathbf{x} - \mathbf{x}'\|_2^2]\right) \end{aligned} \quad (1.23)$$

For the SE kernel, this repeated mapping satisfies

$$k_\infty(\mathbf{x}, \mathbf{x}') - \log(k_\infty(\mathbf{x}, \mathbf{x}')) = 1 + \frac{1}{2}\|\mathbf{x} - \mathbf{x}'\|_2^2 \quad (1.24)$$

The solution to this recurrence has no closed form, but has a similar shape to the Ornstein-Uhlenbeck covariance $k_{OU}(x, x') = \exp(-|x - x'|)$ with lighter tails. Samples from a GP prior with this kernel are not differentiable, and are locally fractal.

1.6.2 When are Deep Kernels Useful Models?

Kernels correspond to fixed feature maps, and so kernel learning is an example of implicit representation learning. Such feature maps can capture rich structure (Duvenaud et al., 2013), and can enable many types of generalization, such as affine invariance in images (Kondor, 2008). ? used a deep neural network to learn feature transforms for kernels, which learn invariances in an unsupervised manner. The relatively uninteresting properties of the kernels derived in this section simply reflect the fact that an arbitrary deep computation is not usually a useful representation, unless combined with learning. To put it another way, any fixed representation is unlikely to be useful unless it has been chosen specifically for the problem at hand.

1.7 Related Work

Prior work on deep GPs Neal (1995) discussed the properties of arbitrarily deep random networks, including those that would give rise to deep GPs. However, deep GPs were first clearly defined and developed by Lawrence and Moore (2007), as a model of hierarchical generative relationships. Deep GPs were first referred to as such in Dami-anou and Lawrence (2013), who developed a variational inference scheme and analyzed the effect of automatic relevance determination in that model.

Other nonparametric neural networks Adams et al. (2010) proposed a prior on arbitrarily deep Bayesian networks. Their architecture has connections only between adjacent layers, and may also be expected to have similar pathologies to those of deep GPs as the number of layers increases.

Deep Density Networks (Rippel and Adams, 2013) were constructed with invertibility in mind, with penalty terms encouraging the preservation of information about lower layers. These models are a promising alternative approach to alleviating the pathology discussed in this paper.

Wilson et al. (2012) introduce GP Regression Networks (GPRN), which define a matrix product of GPs, rather than a composition. The form of the GPRN is

$$\mathbf{y}(\mathbf{x}) = \mathbf{W}(\mathbf{x})\mathbf{f}(\mathbf{x}) \quad \text{with each } f_d, W_{d,j} \stackrel{\text{iid}}{\sim} \mathcal{GP}(\mathbf{0}, \text{SE} + \text{WN}) \quad (1.25)$$

We can easily define a deep GPRN:

$$\mathbf{y}(\mathbf{x}) = \mathbf{W}^{(3)}(\mathbf{x})\mathbf{W}^{(2)}(\mathbf{x})\mathbf{W}^{(1)}(\mathbf{x})\mathbf{f}(\mathbf{x}) \quad (1.26)$$

which might be amenable to a similar analysis to that of section 1.3.

Recurrent networks Bengio et al. (1994) and Pascanu et al. (2012) analyze a related problem with gradient-based learning in recurrent nets, the “exploding-gradients” problem. Specifically, they note that in recurrent neural networks, the size of the training gradient can grow or shrink exponentially as it is back-propagated, making gradient-based training difficult.

Deep kernels Hermans and Schrauwen (2012) construct deep kernels in a time-series setting, constructing kernels corresponding to infinite-size recurrent neural networks (also called Echo State Networks). They also propose concatenating the implicit feature vectors from previous time steps with the current inputs, resulting in an architecture analogous to the input-connected architure proposed by Neal (1995).

Analyses of deep learning Montavon et al. (2010) perform a layer-wise analysis of deep networks, and note that the performance of MLPs degrades as the number of layers with random weights increases. The importance of network architectures relative to learning has been examined by Saxe et al. (2011). Saxe et al. (2013) looked at the dynamics of learning in deep linear models, as a tractable approximation to deep neural networks.

1.8 Conclusions

In this chapter, we attempted to gain insight into the properties of deep neural networks by characterizing the sorts of functions likeley to be obtained under different choices of priors on compositions of functions.

First, we identified deep Gaussian processes as an easy-to-analyze model corresponding to multi-layer preceptrons with nonparametric activation functions. We then showed that representations based on repeated composition of independent functions exhibit a pathology where the representations becomes invariant to all directions of variation but one. Finally, we showed that this problem could be alleviated by connecting the input

to each layer. We also examined properties of deep kernels, corresponding to arbitrarily many compositions of fixed features.

References

- Ryan P Adams, Hanna M Wallach, and Zoubin Ghahramani. Learning the structure of deep sparse graphical models. In *International Conference on Artificial Intelligence and Statistics*, pages 1–8, 2010. (page 17)
- Yoshua Bengio, Patrice Simard, and Paolo Frasconi. Learning long-term dependencies with gradient descent is difficult. *Neural Networks, IEEE Transactions on*, 5(2):157–166, 1994. (page 18)
- Yoshua Bengio, Olivier Delalleau, and Nicolas Le Roux. The curse of highly variable functions for local kernel machines. *Advances in neural information processing systems*, 18:107–114, 2006. ISSN 1049-5258. (page 14)
- Youngmin Cho. *Kernel methods for deep learning*. PhD thesis, University of California, San Diego, 2012. (page 14)
- Andreas Damianou and Neil Lawrence. Deep Gaussian processes. In *Artificial Intelligence and Statistics*, pages 207–215, 2013. (pages 2 and 17)
- David Duvenaud, James Robert Lloyd, Roger Grosse, Joshua B. Tenenbaum, and Zoubin Ghahramani. Structure discovery in nonparametric regression through compositional kernel search. In *Proceedings of the 30th International Conference on Machine Learning*, June 2013. (page 17)
- Robert Gens and Pedro Domingos. Learning the structure of sum-product networks. In *International Conference on Machine learning*, 2013. (page 1)

- Michiel Hermans and Benjamin Schrauwen. Recurrent kernel machines: Computing with infinite echo state networks. *Neural Computation*, 24(1):104–133, 2012. (page 18)
- Imre Risi Kondor. *Group theoretical methods in machine learning*. PhD thesis, Columbia University, 2008. (page 17)
- Neil D Lawrence and Andrew J Moore. Hierarchical Gaussian process latent variable models. In *Proceedings of the 24th international conference on Machine learning*, pages 481–488. ACM, 2007. (page 17)
- Honglak Lee, Chaitanya Ekanadham, and Andrew Ng. Sparse deep belief net model for visual area v2. In *Advances in neural information processing systems*, pages 873–880, 2007. (page 1)
- James Martens. Deep learning via Hessian-free optimization. In *Proceedings of the 27th International Conference on Machine Learning*, pages 735–742, 2010. (page 1)
- JH Maunsell and David C van Essen. The connections of the middle temporal visual area (mt) and their relationship to a cortical hierarchy in the macaque monkey. *The Journal of neuroscience*, 3(12):2563–2586, 1983. (page 10)
- Grégoire Montavon, Dr Braun, and Klaus-Robert Müller. Layer-wise analysis of deep networks with Gaussian kernels. *Advances in Neural Information Processing Systems*, 23:1678–1686, 2010. (page 18)
- Radford M Neal. *Bayesian learning for neural networks*. PhD thesis, University of Toronto, 1995. (pages 4, 10, 17, and 18)
- Razvan Pascanu, Tomas Mikolov, and Yoshua Bengio. Understanding the exploding gradient problem. *arXiv preprint arXiv:1211.5063*, 2012. (page 18)
- Salah Rifai, Grégoire Mesnil, Pascal Vincent, Xavier Muller, Yoshua Bengio, Yann Dauphin, and Xavier Glorot. Higher order contractive auto-encoder. In *Machine Learning and Knowledge Discovery in Databases*, pages 645–660. Springer, 2011a. (page 8)
- Salah Rifai, Pascal Vincent, Xavier Muller, Xavier Glorot, and Yoshua Bengio. Contractive auto-encoders: Explicit invariance during feature extraction. In *Proceedings*

of the 28th International Conference on Machine Learning, pages 833–840, 2011b.

(page 9)

Oren Rippel and Ryan Prescott Adams. High-dimensional probability estimation with deep density models. *arXiv preprint arXiv:1302.5125*, 2013. (page 17)

Andrew Saxe, Pang W Koh, Zhenghao Chen, Maneesh Bhand, Bipin Suresh, and Andrew Y Ng. On random weights and unsupervised feature learning. In *Proceedings of the 28th International Conference on Machine Learning (ICML-11)*, pages 1089–1096, 2011. (page 18)

Andrew M Saxe, James L McClelland, and Surya Ganguli. Dynamics of learning in deep linear neural networks. 2013. (page 18)

Ercan Solak, Roderick Murray-Smith, E. Solak, William Leithead, Carl Rasmussen, and Douglas Leith. Derivative observations in Gaussian process models of dynamic systems, 2003. (page 7)

Andrew Wilson, David A Knowles, and Zoubin Ghahramani. Gaussian process regression networks. In *Proceedings of the 29th International Conference on Machine Learning (ICML-12)*, pages 599–606, 2012. (page 17)